

Computational Fluid Dynamics Methods for Designing the Propeller-Steering Complex of Submarine

Yuriy Korol

Admiral Makarov National University of Shipbuilding, Nikolayev, Ukraine

Abstract: Using the methods and means of computational fluid dynamics, a new method for determining the hydrodynamic characteristics of the propulsion-steering complex of submarines has been developed and implemented. This method is based on a systematic approach to solving problems of mechanical and hydrodynamic interaction of elements of the complex under consideration. On the basis of this technique, the impossibility of scaling the hydrodynamic phenomena that accompany the operation of the elements of the propulsion and steering complex has been proved for the first time. An assessment of the hydrodynamic efficiency of 5 variants of the propulsion and steering complex of the submarine “Zuboff” was carried out.

Key words: Computational fluid dynamics; submarine; propulsion and steering complex; method for assessing hydrodynamic efficiency; influence of geometric characteristics.

1. Introduction

The efficiency of the propulsion and steering complex (PSC) of submarines is usually assessed [2] using the value of the propulsion coefficient and the level of hydro acoustic noise accompanying the operation of its elements. PSC, as you know, consists of 1) an energy source — the main engine; 2) power transmission devices — shafting (reducer); 3) mover; 4) hulls; 5) rudder feather; 6) stock and 7) steering gear. All elements of the PSC are in mechanical, and 3, 4 and 5 also in hydrodynamic interaction, so it is obvious that the process of their design should be carried out on the basis of a systematic approach. Meanwhile, the established practice of designing submarines is based on the decomposition of the system under consideration and the use of the results of physical modeling in experimental pools or wind tunnels to determine the hydrodynamic characteristics

of its elements [7, 10]. The application of computational fluid dynamics (CFD) methods to solving the problems under consideration [1-4, 6, 11, 12], contributing to a very significant reduction in terms and improving the design quality of PSC, demonstrates a high level of accuracy, reliability and information content. However, most of the publications do not go beyond the validation of the applied software products that implement CFD methods based on the results of model physical experiments. Meanwhile, it is the CFD methods that can permanently remove the problem of scalability of hydrodynamic phenomena by implementing the numerical simulation of full-scale objects. To demonstrate the capabilities of CFD methods in this direction, consider the process and the results obtained by the author of the article for determining the hydrodynamic characteristics (HDC) of the elements of the submarine “Suboff” using the Flow Simulation (FS) CAD CAE CAM module of the SolidWorks system.

Corresponding author: Yuriy Korol, Ph.D., Professor, research areas: hydrodynamic improvement of the elements of the propulsion complex of ships. E-mail: yuriy.korol@nuos.edu.ua.

2. Material and Methods

2.1 Determination of the Hydrodynamic Characteristics of the Hull

First of all, according to the data given in [5, 8, 9], 3D models of a full-scale and model submarine were created with a modeling scale of 1/24 and the main geometric characteristics given in Table 1 and the general view shown in Fig. 1.

Further, to determine the HDC of the model hull and nature, we form a computational domain, which is a circular cylinder covering the boat with a diameter of $8D_H$ and a length of $3L$.

In the FS module, we close the ends of the cylinder with plugs and, using the “project master” tool, create a project that simulates the process of fluid flow around the body under the given initial conditions. Then the input data of the project are formed, namely: *boundary conditions* (input, output, ideal and real wall); *the purpose of the calculation* (force along the X - axis, friction force along the X - axis); *mesh* (initial mesh level, minimum clearance); *results*.

The calculation is carried out at different speeds v at the entrance with varying the number of cells in the computational grid (from 0.7 to 2.4 million). According to the results of calculations, it turned out that the number of cells in 1.7 million can be considered sufficient. The obtained dimensionless PSC of the body in the form of dependences of the coefficients of total resistance $C_x(Re)$, frictional resistance $C_{fx}(Re)$ and shape resistance $C_{vpx}(Re)$ on the Reynolds number are shown in Fig. 2.

The dotted curve denotes the Prandtl-Schlichting dependence for the friction drag coefficient of a flat plate.

Table 1 Basic geometric characteristics.

Value	Model	Nature
L - Length, m	4.356	104.607
D_H - Diameter, m	0.508	12.192
Ω - Surface Area, m ²	6.3468	3657.15
Δ - Volume of displacement, m ³	0.706	9757.89



Fig. 1 General view of the 3D model of the hull of the submarine “Suboff”.

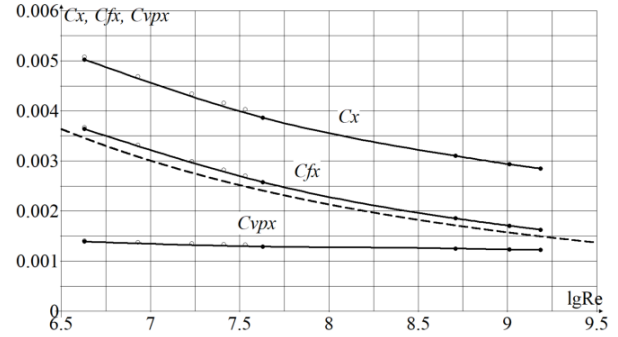


Fig. 2 Dependencies $C_x(Re)$, $C_{fx}(Re)$, $C_{vpx}(Re)$ for model (○) and nature (●).

Analyzing the results presented in this figure, the following should be noted:

- up to numbers $Re \leq 10^{7.5}$, the components of the resistance coefficients for the model and nature are practically the same;
- coefficient of form resistance $C_{vpx} \approx Const$ for $Re \leq 10^{7.5}$;

- the friction drag coefficient curve $C_{fx}(Re)$ is equidistant to the Prandtl-Schlichting curve $C_{f0} = \frac{0.455}{\lg Re^{2.58}}$, but is located about 7% above it.

For a long time, the hypothesis of self-similarity of the coefficient of shape resistance in terms of the Reynolds number was the basis for recalculating the results of a model experiment on nature for submarines. The results obtained indicate that even with an “ideal” model experiment, recalculation to nature will be carried out with a 7% error in the dangerous direction.

2.2 Determination of the Hydrodynamic Characteristics of the Propeller

As is known from [1-4, 6], the model of the submarine under consideration is equipped with an INSEAN E1619 propeller, the main geometric

characteristics of which are given in Table 2 for the model and nature.

Unfortunately, due to the lack of data on the profiling of the blades of this propeller in open print, difficulties arose with the construction of 3D models adequate for the HDC. In this regard, using the author's program GSP3D2017_9, 12 variants of 3D models of propellers with different profile characteristics and distribution laws of the pitch ratio along the radius were created (the appearance of the model is shown in Fig. 3).

The computational domain for the propeller was adopted as a covering cylinder with a diameter of 7 and a length of 10 D . In the FS module, we close the ends of the cylinder with plugs and using the project master tool create a project that simulates the process of flowing a liquid around the propeller under given initial conditions.

A feature of the project is the presence of a cylindrical area of rotation with a given frequency near the propeller. Then the input data of the project are formed, namely: boundary conditions (input, output, ideal and real wall); the purpose of the calculation (force along the X -axis (trust) — T , the moment required for rotation around the X -axis — Q); mesh (level of the initial mesh, minimum gap); results.

Table 2 Main characteristics of the E1619 propeller.

Value	Model	Nature
D - diameter, m	0.262	6.288
z_p - number of blades	7	7
A_E/A_0 - disc ratio	0.608	0.608
d_H/D - rel. hub diameter	0.226	0.226
P/D - pitch ratio	1.15	1.15

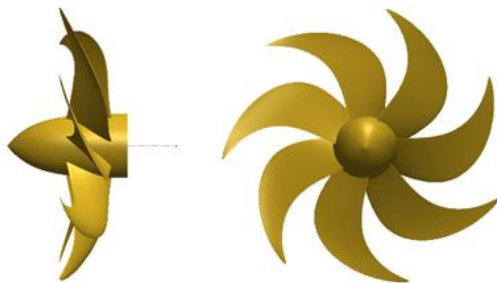


Fig. 3 3D model of the E1619 propeller.

The calculation is carried out at a fixed rotational speed n and different speeds v_p at the input with varying the number of cells in the computational grid (from 0.3 to 1.7 million). According to the results of the calculations, it turned out that the number of cells in 1.2 million can be considered sufficient. Further, according to the obtained and, the calculation of dimensionless HDC was carried out in the form of a

trust coefficient $K_T(J_p) = \frac{T}{\rho n^2 D^4}$, a torque

coefficient $K_Q(J_p) = \frac{Q}{\rho n^2 D^5}$ and efficiency

$\eta_p(J_p) = \frac{K_T}{K_Q} \frac{J_p}{2\pi}$ at fixed values of the relative step

$J_p = \frac{v_p}{nD}$. Comparison of the experimental [8] (dotted

line) and the obtained calculated (solid) action curves shown in Fig. 4 made it possible to choose the propeller screw geometry that is closest to the E1619. Practical coincidence of the results of calculating the propeller action curves in free water for the model and nature indicates their self-similarity in terms of the Reynolds number.

2.3 Determination of the Hydrodynamic Characteristics of the Propulsion and Steering Complex

Let us now consider the principles of building projects and the results of calculations in FS for everything PSC models and natures. First of all, let's add a propeller to the 3D model in such a way that a certain gap remains between the nose end of the hub and the body, excluding their mechanical interaction (see Fig. 5).

The peculiarity of the construction of the project is that the nose end of the cylindrical area of rotation, which covers the propeller, is located in the middle of the above gap (see Fig. 6).

A feature of the calculation at a fixed speed of rotation is the determination of such a speed at which the thrust force of the propeller T is equal to the sum of

the drag and suction forces $R_x + dR$. This is done as follows. For example, let the rotational speed $n = 600$ r/min be set for the model (see Fig. 7).

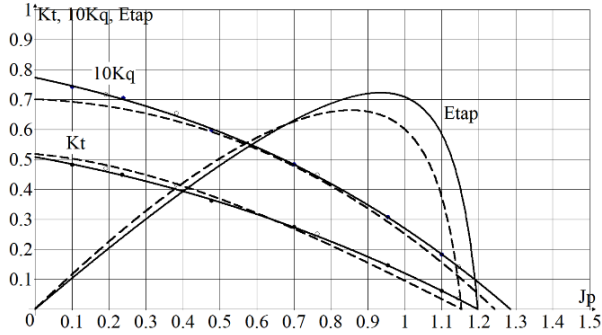


Fig. 4 Propeller action curves for model (○) and nature (●).

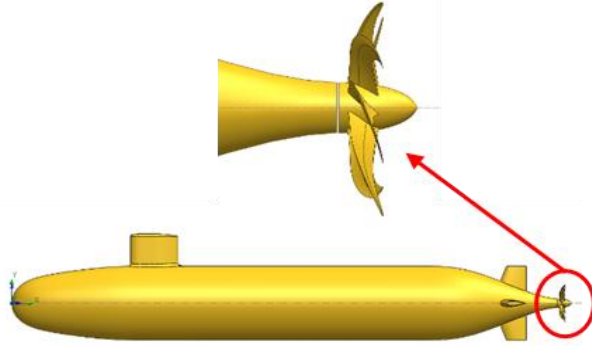


Fig. 5 3D model of the PSC submarine "Suboff".

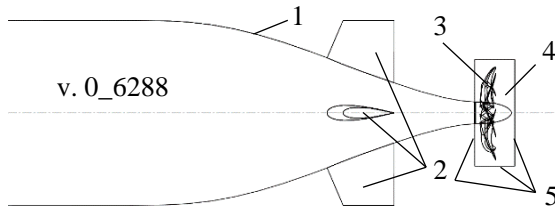


Fig. 6 PSC submarine "Suboff" of the basic version 0_6.288 1. submarine hull; 2. r steering-stabilizer; 3. propeller; 4. area of rotation; 5. sliding surface.

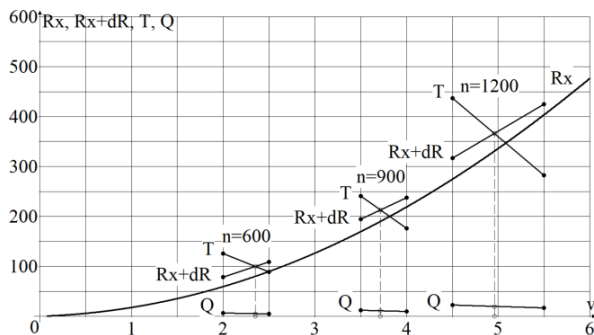


Fig. 7 Determination of the design operating modes of the PSC for the model of the submarine "Suboff".

We set the travel speed $v = 2.0$ m/s and as a result of the calculation we obtain T , $R_x + dR$ and Q (shown by dots), then $v = 2.5$ m/s and, accordingly, the values T , $R_x + dR$ and Q for this speed. Connecting the points of the same name with straight lines, we find the speed v at which $T = R_x + dR$ (the point of intersection) and the moment Q corresponding to this speed. Performing such calculations and constructions for the model and nature (see Fig. 8), we enter their results in Table 3 in the corresponding lines from No. 1-6.

In this table, the suction coefficient t , the relative pitch J , the efficiency η , the relative pitch J_p , the speed in the propeller disk v_p , the coefficient of the associated flow is successively calculated w , thrust coefficient K_T^S and torque coefficient K_Q^S according to the diagram in Fig. 4, thrust T_S and propeller torque Q_S in a homogeneous flow with speed v_p , coefficients of influence of the inhomogeneity of the velocity field and rudders on the thrust i_T and torque i_Q , power required to rotate the propeller without taking into account losses in the shaft line and gearbox P .

2.4 Hydrodynamic Analysis of the PSC Options for the "Suboff" Submarine

The work of the propeller behind the hull in a non-uniform flow is accompanied by the pulsation of forces and moments on the propeller blades, which leads to their vibration. Because of this, an intense hydro acoustic field arises, called the "singing" of the propeller. To reduce the intensity of this field, the

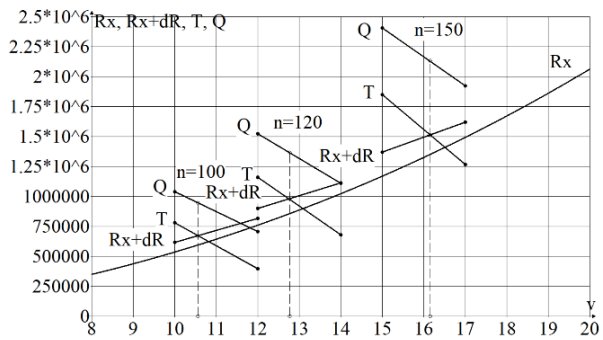


Fig. 8 Determination of the design operating modes of the PSC for the full-scale submarine "Suboff".

propellers of modern submarines have a large number of saber-shaped blades and are located as far as possible from the stern stabilizer rudders. It is this variant of the PSC configuration (0_6.288), shown in Fig. 6, that is the basic one in the study presented below. In the graphs in Figs. 9-10, solid lines show the dependence of the power required for rotation of the propeller and the propulsive ratio on the speed of the basic version. A further decrease in the hydro acoustic field is achieved by installing an annular wing covering the propeller. In the present study, we analyzed the hydrodynamic efficiency of two variants of such wings with the NACA66 airfoil proposed in [5]. The first option has an opening angle of 6.3° , and the second — 10.6° . In addition, each of the options was equipped with seven-bladed propellers with diameters of 6.288 and 4.850 meters, with a relative elongation of the annular wings, respectively, 0.77 and 1.0.

The PSC options are shown in Fig. 6, 11 and the calculation results are shown in Table 4.

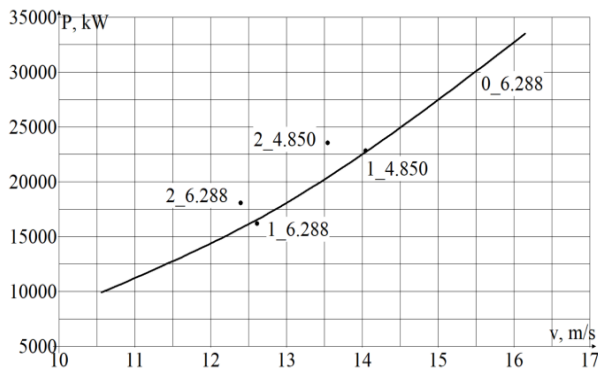


Fig. 9 Dependency $P(v)$.

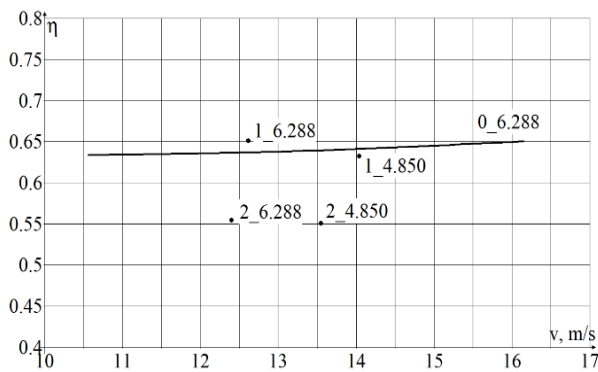


Fig. 10 Dependency $\eta(v)$.

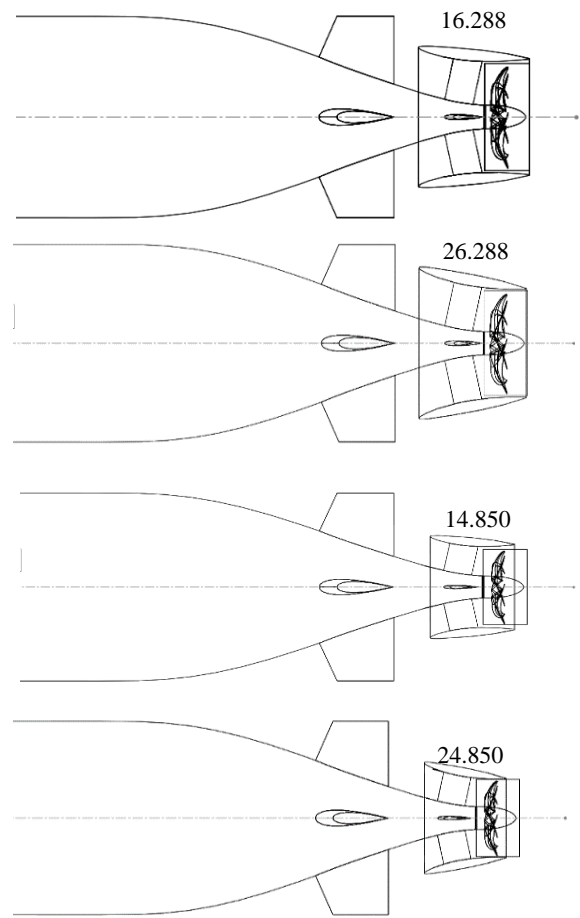


Fig. 11 Options of PSC submarine “Suboff”.

3. Results and Discussion

CFD technology for solving problems of parametric analysis of hydrodynamic characteristics of elements of propulsion and steering systems of surface ships and submarines has firmly entered the practice of their design. In contrast to traditional methods of physical modeling in pilot pools, cavitation and wind tunnels, CFD methods have a number of significant advantages. First of all, this is the absence of the problem of scalability of hydrodynamic phenomena, since the calculation is performed for full-scale objects. Secondly, the time and cost of performing calculations is at least 10 times lower than physical modeling. Thirdly, these methods, possessing significantly greater information content, are devoid of the negative influence of the racks and vibration of

the model on the elastic elements of the model dynamometer. Fourthly, the use of more powerful computer technology will reduce the computation time

so much that it will become possible to use CFD methods not only in analysis problems, but also in synthesis problems.

Table 3 Calculation of the coefficients of interaction of the propeller and the hull of the submarine.

№	Value	Model			Nature		
1	n , rpm	600	900	1200	100	120	150
2	n , rps	10	15	20	1,6667	2.0	2.5
3	v , m/s	2.3520	3.715	4.9575	10.56	12.77	16.15
4	T , N	100,0	212.50	366	670610	979000	1513730
5	$T_e = R$, N	79.91	189.73	330.32	594378	856187	1349875
6	Q , Nm	5.20	10.80	19.56	945950	1365460	2133760
7	$t = \frac{T - T_e}{T}$	0.2009	0.1071	0.0975	0.1137	0.1254	0.1082
8	$J = \frac{v}{nD}$	0.8977	0.9453	0.9461	1.0076	1.0154	1.0273
9	$\eta = \frac{T_e v}{Q 2\pi n}$	0.5752	0.6925	0.6662	0.6336	0.6372	0.6504
10	$J_p(\eta)$	0.6202	0.8125	0.7599	0.7050	0.7106	0.7323
11	$v_p = J_p n D$	1.6249	3.1931	3.9819	7.3885	8.9365	11.5118
12	$w = \frac{v - v_p}{v}$	0.3091	0.1405	0.1984	0.3003	0.3001	0.2872
13	$K_T^S(J_p)$	0.3084	0.2199	0.2454	0.2710	0.2685	0.2584
14	$K_Q^S(J_p)$	0.05293	0.04106	0.04455	0.04800	0.04765	0.04631
15	$T_s = K_T^S \rho n^2 D^4$	145.32	233.14	462.53	1176886	1679014	1679014
16	$Q_s = K_Q^S \rho n^2 D^5$	6.5344	11.40	22.00	1310747	1873637	1679014
17	$i_T = \frac{T}{T_s}$	0.6881	0.9115	0.7913	0.5698	0.5831	0.5995
18	$i_Q = \frac{Q}{Q_s}$	0.7958	0.9474	0.8891	0.7217	0.7288	0.7499
19	$\eta = \frac{i_T (1-t) K_T^S J_p}{i_Q (1-w) K_Q^S 2\pi}$	0.5752	0.6925	0.6662	0.6336	0.6372	0.6504
20	$P = Q 2\pi n$, kW	0.327	1.018	2.458	9910	17158	33520

The methodology and results of the research carried out by the author have been successfully tested at conferences of the Admiral Makarov National University of Shipbuilding [13, 14] and therefore are presented in this article for wider familiarization and discussion by specialists in the hydrodynamics of ships and ocean engineering objects.

The calculation results presented in this article were obtained using the Flow Simulation CAD CAE CAM CFD module of the SolidWorks system installed on a computer with a 4-core 8-thread Intel Core i7-6700HQ processor and 32 GB of RAM. The time spent on the calculation with fixed design parameters is calculated from several hours (1 point on the curves in Fig. 2 and 4) to 15 hours (1 point on

Table 4 Calculation results of PSC options for submarine “Suboff”.

Type ring wings	Value	Signification		
0	D , m	6,288		
	n , rpm	120		
	v , m/s	12	14	12,770
	R , N	759639	$1,02246 \cdot 10^6$	856187
	$R+dR$, N	899681	$1,11222 \cdot 10^6$	979000
	T , N	$1,158439 \cdot 10^6$	679174	979000
	Q , Nm	$1,524681 \cdot 10^6$	$1,11001 \cdot 10^6$	$1,36546 \cdot 10^6$
	η	-	-	0.6372
	P , kW	-	-	17159
1	D , m	6,288		
	n , rpm	120		
	v , m/s	12	14	12,611
	R , N	759639	$1,02246 \cdot 10^6$	835779
	$R+dR$, N	901190	$1,19873 \cdot 10^6$	991499
	T , N	$1,10895 \cdot 10^6$	724805	991499
	Q , Nm	$1,35057 \cdot 10^6$	$1,01708 \cdot 10^6$	$1,28810 \cdot 10^6$
1	η	-	-	0,6511
	P , kW	-	-	16187
2	D , m	6,288		
	n , rpm	120		
	v , m/s	12	14	12,396
	R , N	759639	$1,02246 \cdot 10^6$	808574
	$R+dR$, N	$1,10942 \cdot 10^6$	$1,54992 \cdot 10^6$	$1,19608 \cdot 10^6$
	T , N	$1,26371 \cdot 10^6$	925491	$1,19608 \cdot 10^6$
	Q , Nm	$1,49374 \cdot 10^6$	$1,20573 \cdot 10^6$	$1,43750 \cdot 10^6$
	η	-	-	0,5549
	P , kW	-	-	18064
1	D , m	4.850		
	n , rpm	200		
	v , m/s	12	14	14,040
	R , N	759639	$1,02246 \cdot 10^6$	$1,02812 \cdot 10^6$
	$R+dR$, N	906961	$1,14810 \cdot 10^6$	$1,15538 \cdot 10^6$
	T , N	$1,53901 \cdot 10^6$	$1,15375 \cdot 10^6$	$1,15538 \cdot 10^6$
	Q , Nm	$1,34304 \cdot 10^6$	$1,09003 \cdot 10^6$	$1,09003 \cdot 10^6$
	η	-	-	0,6323
	P , kW	-	-	22829
2	D , m	4.850		
	n , rpm	200		
	v , m/s	12	14	13,544
	R , N	759639	$1,02246 \cdot 10^6$	959072
	$R+dR$, N	933238	$1,21127 \cdot 10^6$	$1,146595 \cdot 10^6$
	T , N	$1,55625 \cdot 10^6$	$1,10260 \cdot 10^6$	$1,146595 \cdot 10^6$
	Q , Nm	$1,25850 \cdot 10^6$	$1,05968 \cdot 10^6$	$1,125716 \cdot 10^6$
	η	-	-	0,5509
	P , kW	-	-	23577

the curves in Figs. 6-10). Obviously, the estimated time can be significantly reduced by using computers with 32 or 64 cores.

The calculation results of the coefficient $C_x(\text{Re})$ shown in Fig. 2, indicate the sufficient correctness of the widely used method of recalculation from model to field; however, the calculated data must be considered more accurate, since they do not contain errors from the influence of the dynamometer stands and vibration of the model in the flow.

In Fig. 4 shows one more proof of the self-similarity of the dimensionless characteristics of the propeller in terms of the Strouhal number ($Sh = J_P$), which undoubtedly indicates the correctness of the results obtained.

The most interesting results were obtained when calculating the propulsion-steering complexes for the model (Fig. 7, Table 3) and nature (Fig. 8, Table 3). The condition for the joint operation of the elements of the propulsion and steering complex at a given propeller rotational speed is the point of intersection of the thrust $T(v)$ and resistance curves, taking into account the suction force $(Rx+dR)(v)$, which determines the design speed and the moment required to rotate the propeller. The dependences of the associated flow $w(J_P)$ and suction coefficients obtained $t(J_P)$ on the models were usually extrapolated to the values of the full-scale relative flows. The data in Table 3 convincingly indicate the incorrectness of this approach and the inexpediency of performing model tests.

The proposed method made it possible to determine the hydrodynamic efficiency of 5 variants of the propulsion and steering complex of the submarine "Suboff", presented in Fig. 9, 10 and in Table 4, which can serve as a basis for making a substantiated design decision.

4. Conclusion

Analyzing the results obtained, one can come to the following conclusions:

1) an attempt to ensure equality of relative steps (8th row of Table 3) for the model and nature turned out to be unsuccessful, since it is physically impracticable;

2) the proposed method for determining the interaction coefficients of the elements of the PSC allowed for the first time to calculate not only w and t , but i_T also i_Q ;

3) CFD methods make it possible to determine the characteristics of submarine PSCs necessary for the design without using any model physical experiments, which can significantly improve the quality, reduce material costs and shorten the development time of projects.

References

- [1] S. Burunsuz, M. C. Özden, Y. A. Özden and İ. H. Helvacioğlu, Four quadrant thrust and torque prediction of INSEAN E-1619 generic submarine propeller for submarine maneuvering simulations, in: *Fifth International Symposium on Marine Propulsors smp'17*, Espoo, Finland, June 2017, pp. 1-7.
- [2] N. Chase, Simulations of the DARPA Suboff submarine including self-propulsion with the E1619 propeller, thesis, University of Iowa, 2012, pp.1-50.
- [3] C. Delen, S. Sezen and S. Balı, Computational investigation of self-propulsion performance of DARPA SUBOFF vehicle, *Tamap Journal of Engineering* 4 (2017) 1-12.
- [4] Fillipe Rocha Esteves, Gustavo de Goes Gomes, Eduardo Tadashi Katsuno and João Lucas Dozzi Dantas, Simulation of DARPA Suboff model propeller-hull interaction, in: *27º Congresso Internacional de Transporte Aquaviário, Construção Naval e Offshore*, Rio de Janeiro/RJ, 23-25 de outubro de, (2018). p.1-9.
- [5] N. C. Groves, T. T. Huang and M. S. Chang, Geometric characteristics of DARPA Suboff (DTRC MODEL NOS. 5470 and 5471): DTRC/SHD 1298-01, 1989, pp. 1-75.
- [6] F. Jianga, Z. Zhangb, J. Cheng and Y. Ge, Large Eddy Simulation of DARPA SUBOFF for $\text{Re} = 2.65 \times 10^7$, in: *Proceedings of the Eighth International Workshop on Ship Hydrodynamics*, Seoul, Korea, September 23-25, 2013, pp. 1-5.
- [7] Joubert Peter, Some Aspects of Submarine Design Part 1: Hydrodynamics, Victoria 3207 Australia: DSTO Platforms Sciences Laboratory 506 Lorimer St Fisherman's Bend, 2004.

- [8] H. L. Liu and T. T. Hang, Summary of DARPA Suboff Experimental Program Data, CRDKNSWC/HD-1298-11 June 1998, pp. 1-28.
- [9] M. Mackay, The standard submarine model: A survey of static hydrodynamic experiments and semi empirical predictions, Defense R&D Canada – Atlantic: Technical Report DRDC Atlantic TR 2003-079, 2003.
- [10] M. Renilson, Submarine Hydrodynamics, Launceston TAS Australia: Springer Briefs in Applied Sciences and Technology, 2015.
- [11] S. Toxopeus, Viscous-flow calculations for bare hull DARPA SUBOFF submarine at incidence, *International Shipbuilding Progress* 55 (2008) 227-251.
- [12] Yung-An Chu, Chun-Ta Lin, Ching-Yeh Hsin and Ya-Jung Lee, Numerical Analysis of Propulsion for Submarine with Highly Skewed Propeller, in: *Proceedings of 8th PAAMES and AMEC 2018*, Busan, 9-12 October, 2018.
- [13] Ю. М. Король, Методы вычислительной гидродинамики в задачах проектирования движительно-рулевого комплекса подводных лодок. Миколаїв, НУК, Сучасні технології проектування, побудови, експлуатації і ремонту суден, морських технічних засобів і інженерних споруд. Матеріали всеукраїнської науково-технічної конференції з міжнародною участю, 2019, pp. 30-38.
- [14] Ю. М. Король, Гидродинамический анализ вариантов движительно-рулевого комплекса подводной лодки Suboff, Инновации в судостроении и океанотехнике, Материалы X международной технической конференции, Национальный университет кораблестроения имени адмирала Макарова, Николаев, Украина, 2019, pp. 43-47.